



## Benign approach for methyl-esterification of oxygenated organic compounds using TBHP as methylating and oxidizing agent

Topi Ghosh<sup>a</sup>, Prakash Chandra<sup>b</sup>, Akbar Mohammad<sup>a</sup>, Shaikh M. Mobin<sup>a,b,c,\*</sup>

<sup>a</sup> Discipline of Chemistry, Indian Institute of Technology Indore, Simrol, Khandwa Road, Indore, 453552, India

<sup>b</sup> Discipline of Metallurgy Engineering and Material Science, Indian Institute of Technology Indore, Simrol, Khandwa Road, Indore, 453552, India

<sup>c</sup> Discipline of Biosciences and Bio-Medical Engineering, Indian Institute of Technology Indore, Simrol, Khandwa Road, Indore, 453552, India



### ARTICLE INFO

#### Keywords:

Methyl-esterification  
Oxygenates  
Pd/Cu<sub>2</sub>Cl(OH)<sub>3</sub> nanocatalyst  
TBHP dual role  
Recyclable nanocatalyst

### ABSTRACT

Methyl-esterification of oxygenates such as alcohols, aldehydes and carboxylic acids were carried out by employing copper and copper/palladium based catalysts using TBHP. In this reaction, TBHP plays dual role as oxidizing and methylating agent. Cu and Cu-Pd based nanoparticles (NPs) were prepared by wet chemical method using CuCl or PdCl<sub>2</sub> by engaging “green solvent” water and dextrose as eco-friendly and renewable reagents. The NPs were fully characterized using various physicochemical techniques such as XRD, SEM, TEM and EDAX. XRD spectra of synthesized NPs confirmed the formation of CuO and Pd/Cu<sub>2</sub>Cl(OH)<sub>3</sub>. HRTEM analysis of CuO confirmed uniform cube-shaped morphology with particle size of 25–30 nm. Whereas, HRTEM of Pd/Cu<sub>2</sub>Cl(OH)<sub>3</sub> showed 5–10 nm Pd NPs uniformly dispersed over Cu<sub>2</sub>Cl(OH)<sub>3</sub> surface. Excellent catalytic activity was obtained for the conversion of benzaldehyde to methyl benzoate with 92% selectivity using Pd/Cu<sub>2</sub>Cl(OH)<sub>3</sub> nanocatalyst. Other oxygenates such as aldehydes, alcohols and carboxylic acids were also obtained with high conversion and selectivity for desired methyl esters.

### 1. Introduction

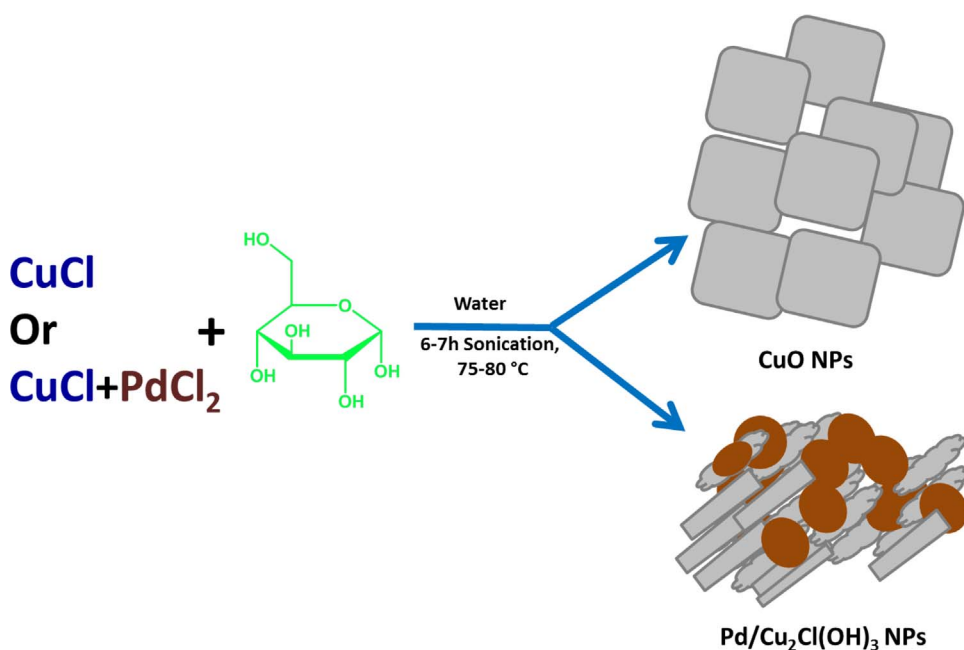
Methylation of organic substrates is most fundamental as well as substantial transformation in synthetic organic chemistry, methyl group is one of the most significant functionality present on organic compounds [1]. Presence of methyl group greatly alters the pharmacological activity of biomolecules for multivariable biological phenomenon [2–6]. Conventionally frequently used methylating sources are methyl iodide, dimethyl sulfate, diazomethane, methyl carbonate and several methyl organometallic reagents [7]. The major class of methylations, that is, C-, N- and O-methylation have been investigated by the researchers. C-methylation includes methylation of aryl and vinyl halides, methylation of C–H bond, decarboxylative methylation of  $\alpha$ ,  $\beta$ -unsaturated compounds. N- and O-methylation includes methylation of N-containing compounds and O-methylation includes methylation of carboxylic acid [1].

Amongst all O-methylation of alcohols, aldehydes and carboxylic acids to produce their respective methyl esters results in the synthesis of the significant class of chemical compounds and building block in different natural product and polymers. Methyl esterification is one of the most fundamental transformations in organic synthesis [8,9]. There are several naturally occurring biologically active methyl esters such as

methyl jasmonate and biphenyl dicarboxylate which have medicinal applications. Fatty acid methyl esters are another significant class of versatile chemicals having potential applications in lubricants, metal working fluids, solvents fuels, surfactants, polymers, coatings and food. These fatty acid methyl esters are also used as “green solvents” because they are biodegradable, non-toxic and produce low volatile organic compounds (VOCs).

The common synthetic routes to methyl esters are the reactions of alcohols, aldehydes, acids with methanol in the presence of acid or base [7,10,11]. Mechanistically, the oxidation of hemiacetal intermediate, *in-situ* generated from the condensation of alcohol with aldehyde, is the key step for these conversions [12–15]. Transition metals such as Al, Au, Ru, Ir or Zn show high catalytic efficiency for the cross-esterification reaction of these organic substrates [16–19]. The Tishchenko reaction of direct conversion of aldehydes to the corresponding esters represents the most effective method for the synthesis of esters. However, above said reactions results in the generation of undesired side products such as acids and alcohols with a very limited substrate scope [20]. Methyl esterification can also be synthesized by C–H functionalization resulting into C–O bond formation in presence of CO and methanol [21], C–H activation of alkoxycarbonylation of aryl (C–H  $sp^2$ ), alkenyl (C–H  $sp^2$ ), alkynyl (C–H  $sp$ ), alkyl (C–H  $sp^3$ ) with methanol and other

\* Corresponding author at: Discipline of Chemistry, Indian Institute of Technology Indore, Simrol, Khandwa Road, Indore 453552, India.  
E-mail address: [xray@iiti.ac.in](mailto:xray@iiti.ac.in) (S.M. Mobin).



**Scheme 1.** Schematic representation for the synthesis of CuO and Pd/Cu<sub>2</sub>Cl(OH)<sub>3</sub> NPs.

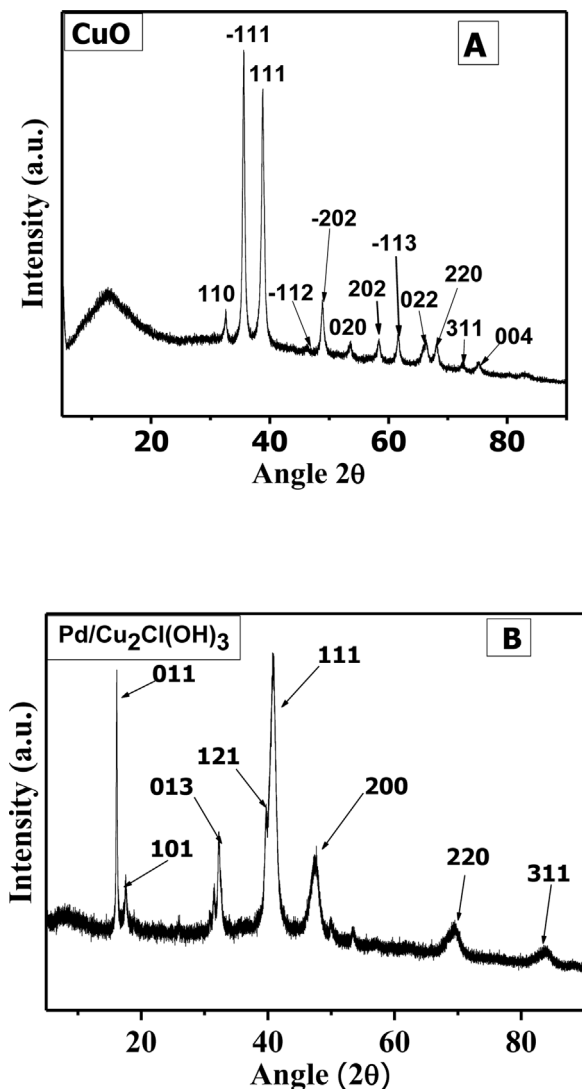


**Fig. 1.** XRD spectra of CuO NPs (A); Pd/Cu<sub>2</sub>Cl(OH)<sub>3</sub> NPs (B).

esterifying agents such as methyl chloroformate [22],  $\alpha$ -ketoesters [23], CO<sub>2</sub> [24] and activation of alkenes with methyl formate *via* C–H activation of methyl formate etc. has been used extensively for esterification reaction. Hydroacylation of carbonyl compounds *via* aldehydic C–H bond activation with methanol has also been investigated for methyl esterification reaction [8]. Stereoselective alkoxy carbonylation of unactivated C(sp<sup>3</sup>)–H bond with alkyl chloroformates using Pd(II)/(IV) catalysis has been performed for esterification reaction [25]. To the best of our knowledge, there are very few examples of Cu-catalyzed direct esterification of alcohols, aldehydes, carboxylic acid with tert-Butyl hydroperoxide as oxidant as well as the methylating agent. Mao *et al.* [26] have reported methyl esterification using TBHP as oxidant and C-methylating agent and Cu-quinoline complex as a catalyst and tetrabutylammonium iodide (TBAI) as an additive. But, the aforementioned catalytic systems are not recyclable and uses toxic solvents such as N, N-dimethylformamide(DMF) or dimethylsulfoxide(DMSO). Li *et al.* [7] have investigated aforementioned reaction using copper fluoride (CuF<sub>2</sub>) as a catalyst for oxidative methyl esterification. However, both the aforementioned protocols utilize homogeneous Cu-based catalyst and TBAI as an additive used resulting in the generation of the copious amount of waste materials. Recently, there is also a report on the application of Cu-MOF as an effective heterogeneous catalyst for methyl esterification reaction. However, synthesis of such MOFs is complicated, therefore a benign protocol for synthesis of methyl ester using TBHP as a methylating as well as the oxidizing agent is a need of the hours [27].

To address the aforementioned issue, the present work demonstrates a step ahead for more a facile approach for chemical manufacturing by employing Cu-nanocatalyst for oxidative methyl-esterification reaction. The common applications of copper or copper oxide NPs revolves around four types of chemical reactions, namely reduction, hydrolysis, condensation, and oxidation [28]. On the basis of the previous literature reports, the methods for synthesizing CuO NPs can be classified as (a) chemical, [29] (b) electrochemical, [30] (c) photochemical, [31] (d) sonochemical, [32], and (e) thermal treatment method [33]. The chemical treatment method is most frequently utilized and is further classified into wet chemical, [34] microwave assisted, reverse micelle [35] and ionic liquid assisted [36] methods depending on materials, reaction environment and synthetic methodology used. “Wet chemical” technique is long established method mostly involves reduction of metal salts such as copper(II) acetylacetone, CuCl<sub>2</sub>, Cu(NO<sub>3</sub>)<sub>2</sub>, etc. in

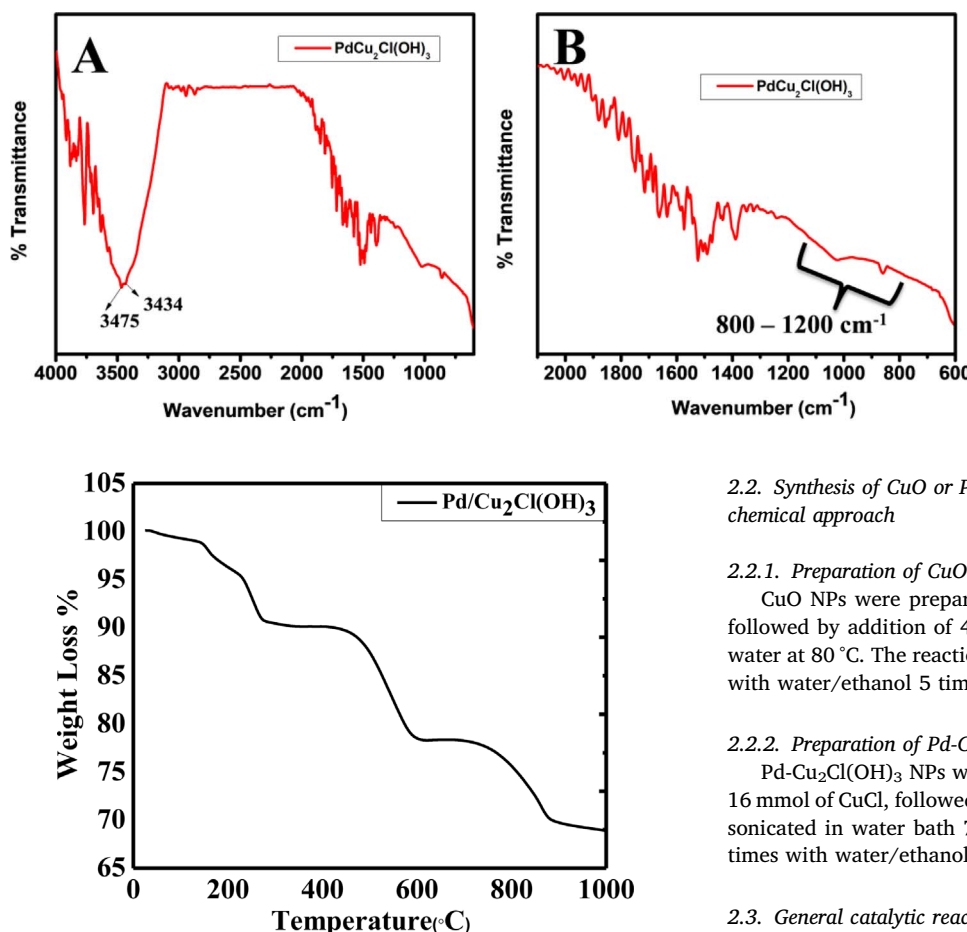


Fig. 3. Thermogravimetric analysis of as-prepared nanoscaled Pd/Cu<sub>2</sub>Cl(OH)<sub>3</sub> (total sample weight: 6.541 mg).

presence of solvent; reducing agents sodium borohydride [37], hydrazine [38], ascorbic acid [39], D-glucose [40] etc.

There are several reports for the “wet chemical reduction” of cupric salts to metallic copper, Cu<sub>2</sub>O or CuO NPs. Herein, the present manuscript we utilize “Wet chemical” method for synthesis of CuO NPs via oxidation of copper(I) chloride (CuCl) using dextrose as oxidizing agent and water as “green solvent”. Green, eco-friendly and benign method following 12 principles of green chemistry have been exhaustively addressed in this work by using water as “green solvent” and dextrose as renewable eco-friendly redox agent [41–43]. Replacement of hazardous organic solvents with water benign solvents, and renewable materials such as dextrose are key issues in the nanomaterials science field while considering a green synthetic strategy. The prime objectives of the present work is to use green, eco-friendly and more benign approach to the oxidative methyl-esterification reaction using robust, heterogeneous and recyclable copper based nanocatalyst. The present catalyst also has an edge over earlier reported catalyst in terms of homogeneous, non-recyclable, toxic solvents or catalytic material and complicated synthesis route.

## 2. Experimental

### 2.1. Materials

Commercially available starting materials were used as received. CuCl and dextrose were purchased from Merck India. Organic alkene, aldehydes, acids and alcohols were reagent purchased from Sigma Aldrich and other reagent grade solvents were used as received.

## 2.2. Synthesis of CuO or Pd-Cu<sub>2</sub>Cl(OH)<sub>3</sub> nanoparticles (NPs) via wet chemical approach

### 2.2.1. Preparation of CuO NPs

CuO NPs were prepared by dissolving 16 mmol of CuCl (1.584 g), followed by addition of 4.0 g dextrose in 100 ml of distilled deionized water at 80 °C. The reaction was continued for 7 h followed by washing with water/ethanol 5 times and water 5 times.

### 2.2.2. Preparation of Pd-Cu<sub>2</sub>Cl(OH)<sub>3</sub> NPs

Pd-Cu<sub>2</sub>Cl(OH)<sub>3</sub> NPs were prepared by dissolving 4 mmol PdCl<sub>2</sub> and 16 mmol of CuCl, followed by addition of 4.0 g dextrose in 100 ml water sonicated in water bath 75–80 °C upto 6 h, centrifuged and washed 5 times with water/ethanol and 5 times with water.

## 2.3. General catalytic reaction

The liquid phase catalytic oxidation was carried out in a (50 ml one necked) round bottom flask equipped with a magnetic stirrer and immersed in a thermostat controlled oil bath. The flask was charged with substrate (1 mmol), oxidant TBHP 70 wt% in H<sub>2</sub>O, 700 mg (8 eq), 10 mg of catalyst, K<sub>2</sub>CO<sub>3</sub> (44 mg) and solvent acetonitrile: water (3:1) 4 ml. All the reactions were carried out at 100 °C, 24 h. Samples were periodically withdrawn and analyzed on Shimadzu GC-MS (Spectra S1-S23).

## 2.4. Physio-chemical characterizations

Powder X-ray diffraction studies were carried out on RigakuSmartLab X-ray diffractometer using CuK $\alpha$  radiation (1.54 Å). Infrared spectra were performed with a Bio-Rad FTS 3000MX instrument using KBr pellets. Thermogravimetric analysis (TGA) were performed on METTLER TOLEDO (TGA/DSC 1) using software STAR<sup>e</sup> System. H<sub>2</sub>-TPR analysis and CO titration was carried out in (Quantachrome). Temperature-programmed reduction (TPR) was performed in a micro-flow reactor (Quantachrome, Autosorb iQ2). To carry out the experiment, a catalyst sample (175 mg) was heated from 50 °C to 600 °C at a rate of 10 °C/min and fed with 80 ml/min of gas mixture containing 5% H<sub>2</sub> and 95% N<sub>2</sub>. CO titration was carried out on Quantachrome, Autosorb iQ2 to analyze the Pd dispersion on the catalysts surface using carbon monoxide as the adsorbate and Pd as the adsorbent at ambient temperature and pressure. FE-SEM attached with EDAX was done using Supra55 Zeiss Field-Emission Scanning Electron Microscope. Transmission Electron Microscopy was carried on FEI Tecnai G2 12 Twin TEM. XPS analysis of fresh and spent catalyst (Pd/Cu<sub>2</sub>Cl(OH)<sub>3</sub>) was performed using X-ray Photoelectron Spectroscopy (XPS) with Auger Electron Spectroscopy (AES) Module: Model/Supplier: PHI 5000 Versa Prob II, FEI Inc. Identification of the products of the carried out using Shimadzu GC-MS equipped with QP2010 mass spectrometer and RTX-5 tubular diphenyl dimethyl polysiloxane

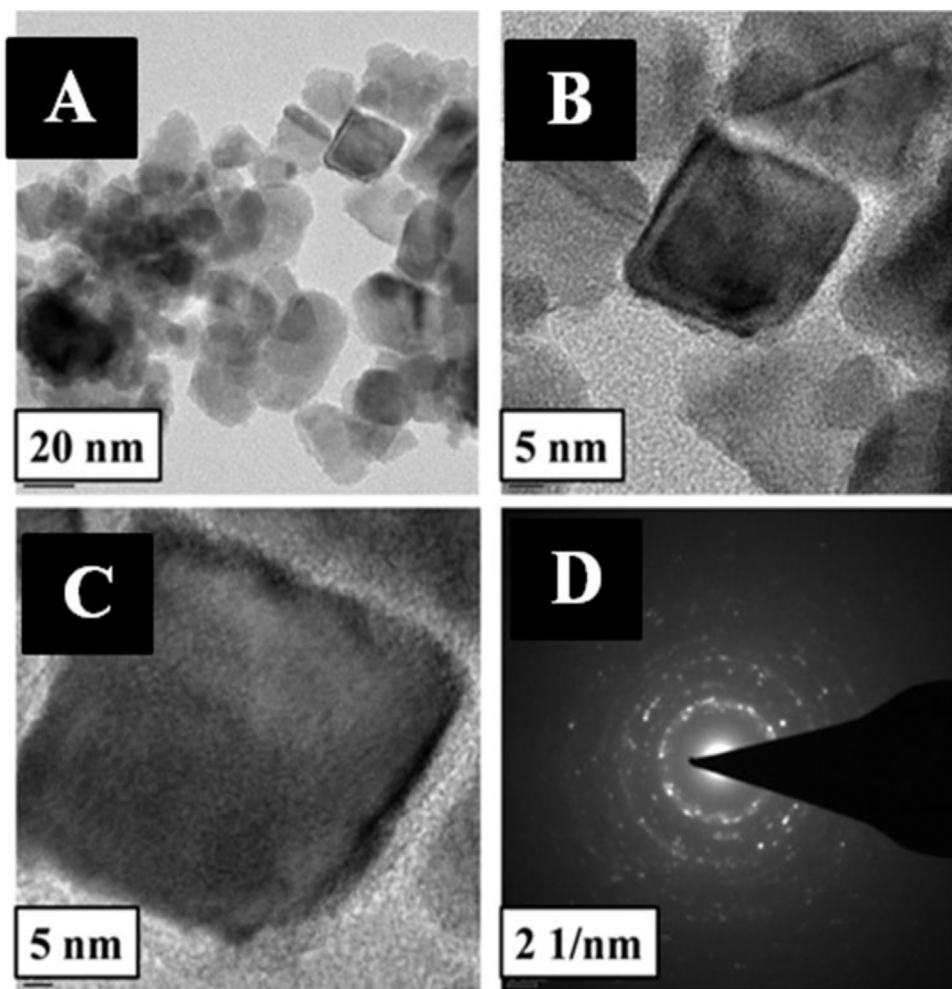


**Fig. 4.** HRTEM image of CuO nanocatalyst at 20 nm (A); 5 nm (B); 5 nm (C) magnification; SAED pattern of CuO nanocatalyst at 2 1/nm (D).

capillary column 30 m long, 0.25 mm diameter and df value of 1.0  $\mu\text{m}$ .

### 3. Results and discussion

#### 3.1. Characterization of the catalytic materials

Synthesis of copper oxide and Cu-Pd based nanoparticles (NPs) were carried out using “wet chemical method” as shown in [Scheme 1](#).

$$B\left(\frac{2\theta}{\lambda}\right) = \frac{K\lambda}{L \cos \theta}$$

The XRD patterns of CuO NPs showed the monoclinic structure with  $2\theta = 32.1^\circ, 35.2^\circ, 39.1^\circ, 48.3^\circ, 58.2^\circ, 62^\circ, 66.2^\circ, 68.3^\circ$  and  $75.2^\circ$  which can be readily indexed as 100, 11-1, 111, 200, 20-2, 002, 113, 220 and 311 planes, respectively ([Fig. 1A](#)) [44]. Particle size was calculated using Scherrer's equation.

Particle size of the CuO nanoparticles calculated using Scherrer's equation was found to be 30 nm. The XRD pattern of Pd-nanoparticles supported on copper based NPs [Pd/Cu<sub>2</sub>Cl(OH)<sub>3</sub>] is shown in [Fig. 1B](#). The observed intense Bragg reflection peaks at  $40.9^\circ, 47.9^\circ, 69.4^\circ, 84.2^\circ$  and  $87^\circ$  representing the 111, 200, 220, 311 and 222 respectively, was compared and confirmed the formation of palladium NPs (JCPDS standard 05-0681) [45,46]. Moreover, the four main diffraction peaks at  $2\theta = 16.4^\circ, 32.1^\circ, 39.6^\circ$  and  $50.3^\circ$  are ascribed to the phase of chinoatacamite Cu<sub>2</sub>Cl(OH)<sub>3</sub> (JCPDS 50-1559) ([Fig. 1B](#)) [47]. Particle size of Pd/Cu<sub>2</sub>Cl(OH)<sub>3</sub> calculated using Scherrer's equation was found to be 12 nm.

In the FT-IR spectrum of Pd/Cu<sub>2</sub>Cl(OH)<sub>3</sub> ([Fig. 2](#)), the two absorption

peaks at  $3447$  and  $3358\text{ cm}^{-1}$  are ascribed to the hydroxyl stretching modes  $\nu_1(\text{O1-H1})/\nu_1(\text{O2/3-H2/3})$  of the Cu<sub>2</sub>Cl(OH)<sub>3</sub>, the IR bands between  $800$ – $1200\text{ cm}^{-1}$  can be attributed to the  $\delta_1$  and  $\nu_1$  (Cu—O—H) vibrations [48].

Thermogravimetric analysis (TGA) was performed to determine thermal characterisation of Pd/Cu<sub>2</sub>Cl(OH)<sub>3</sub> ([Fig. 3](#)). Here, decomposition of Pd/Cu<sub>2</sub>Cl(OH)<sub>3</sub> is observed with 9.5 wt% (0.621 mg) weight-loss below  $300^\circ\text{C}$ , followed by 12 wt% (0.784 mg) up to  $600^\circ\text{C}$  and finally 9.3% (0.61 mg) weight loss from  $600$ – $900^\circ\text{C}$ . This weight loss is due to the dissociation of HCl and water molecules [49]. XRD, FT IR and TGA analysis corroborate formation of Cu<sub>2</sub>Cl(OH)<sub>3</sub> in Pd/Cu<sub>2</sub>Cl(OH)<sub>3</sub> [47–50].

SEM micrograph shows uniformly dispersed CuO and Pd-Cu<sub>2</sub>Cl(OH)<sub>3</sub> NPs ([Fig. S1](#) A-D). EDAX analysis of Pd-Cu<sub>2</sub>Cl(OH)<sub>3</sub> is shown in [Fig. S2](#) A-F, Table S1. The EDX spectrum obtained from samples indicated that Pd/Cu<sub>2</sub>Cl(OH)<sub>3</sub> nanoparticles contain the elemental Pd, Cu, O and Cl [48]. EDX analysis shows that the atom ratio of Cu and Cl is nearly 2:1, indicating that the composition of the as-prepared samples is Cu<sub>2</sub>Cl(OH)<sub>3</sub> (Table S1). EDAX analysis confirms the presence of Pd, Cu and Cl in Pd-Cu<sub>2</sub>Cl(OH)<sub>3</sub> [[Fig. S2](#) (A-F) and Table S1]. HRTEM image of CuO NPs also reveals the formation of uniformly dispersed size and cube-shaped NPs of 30–40 nm dimensions ([Fig. 4](#)). Selected area electron diffraction (SAED) performed on samples of CuO NPs aggregate obtained from HR-TEM showed a concentric ring pattern indicating crystalline nature of the material ([Fig. 4](#)). HRTEM images of Pd-Cu<sub>2</sub>Cl(OH)<sub>3</sub> NPs are presented in ([Fig. 5](#)). HRTEM of as-prepared NPs show formation of uniformly dispersed Pd NPs (10–15 nm) over Cu<sub>2</sub>Cl(OH)<sub>3</sub> surface ([Fig. 5A-C](#)). SAED pattern of Pd-Cu<sub>2</sub>Cl(OH)<sub>3</sub>

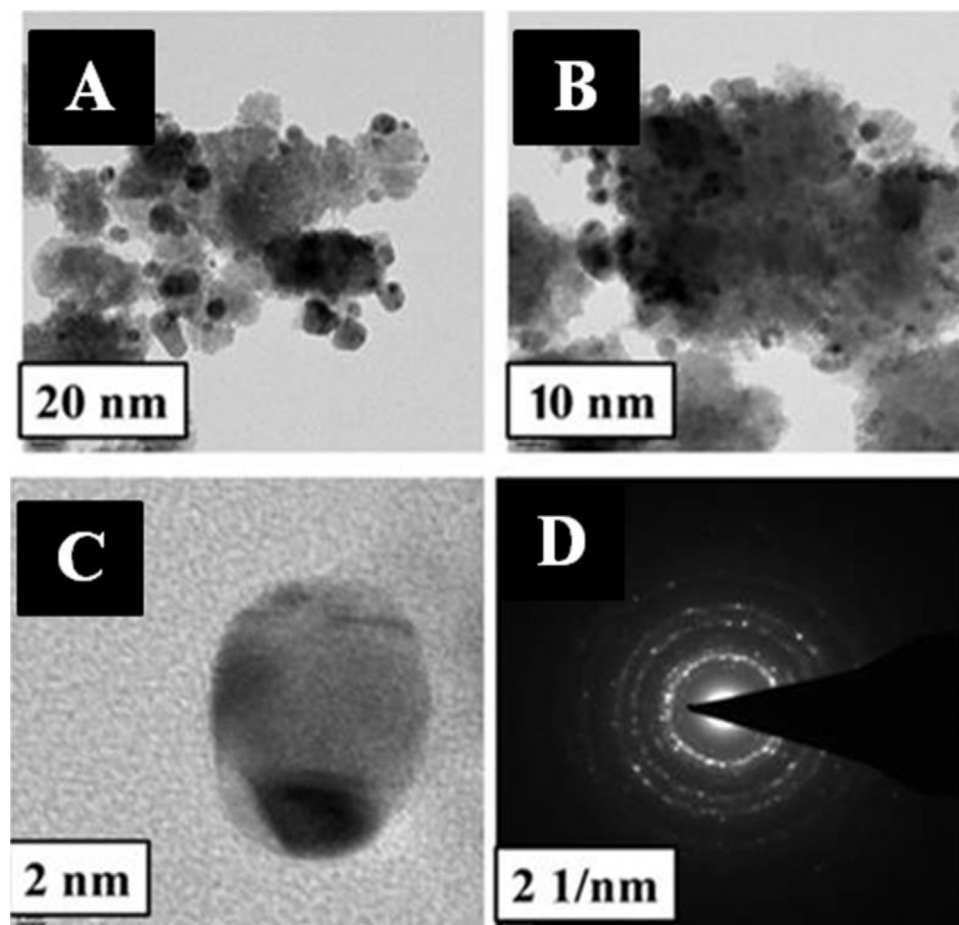


Fig. 5. HRTEM image of  $\text{Pd-Cu}_2\text{Cl}(\text{OH})_3$  nanocatalyst at 20 nm (A); 10 nm (B); 2 nm; (C) SAED image of  $\text{Pd-Cu}_2\text{Cl}(\text{OH})_3$  nanocatalyst at 2 1/nm (D).

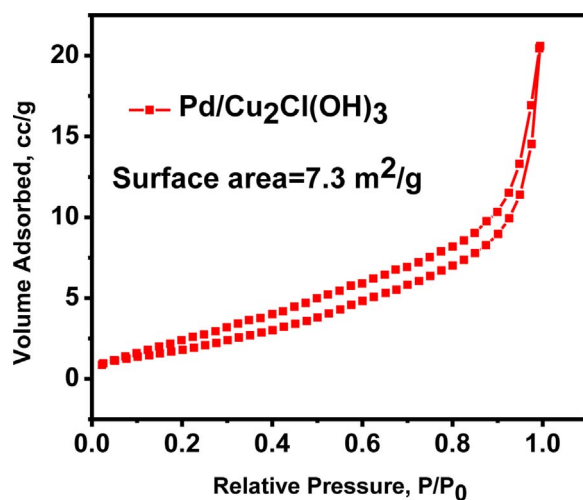


Fig. 6. Brunauer–Emmett–Teller (BET) surface area of the  $\text{Pd/Cu}_2\text{Cl}(\text{OH})_3$ .

presents concentric rings revealing formation of crystalline material (Fig. 5D).

The Brunauer–Emmett–Teller (BET) surface area and pore diameters of the  $\text{Pd/Cu}_2\text{Cl}(\text{OH})_3$  were determined by  $\text{N}_2$  adsorption measurements (see. Surface area of the catalyst calculated from BET measurements was  $7.3 \text{ m}^2/\text{g}$ . (Fig. 6). To determine the presence of Pd nanoparticles on the catalyst surface SEM-EDAX analysis was performed and confirmed the presence of Pd atoms on the catalyst surface [See Fig. S2 (F) and Table S1].

CO titration was also performed to analyze the Pd dispersed over the

$\text{Cu}_2\text{Cl}(\text{OH})_3$  surface. CO titration study reveal that surface area of Pd dispersed over  $\text{Cu}_2\text{Cl}(\text{OH})_3$  have surface area  $1.04 \text{ m}^2/\text{g}$  with average crystallite size of 182.5 nm. As for the well-reduced  $\text{Pd/Cu}_2\text{Cl}(\text{OH})_3$  show particle sizes were estimated by CO chemisorptions under the assumption that CO was linearly adsorbed on  $\text{Pd/Cu}_2\text{Cl}(\text{OH})_3$  surface and the estimated sizes were actually larger than the particle size monitored using TEM or XRD due to surface carbonyl formation with more than one CO molecule being adsorbed per surface Pd atom [51].

The high-resolution XPS spectra in Fig. 7 and 8 reveal the survey of the fresh and spent  $\text{Pd-Cu}_2\text{Cl}(\text{OH})_3$  nanocatalysts. High resolution XPS spectra of Pd-region reveals a doublet structure each with two pairs of peaks at 335.6 and 340.9 eV representing Pd  $3d_{3/2}$  and Pd  $3d_{1/2}$ , respectively for bulk Pd(0) (Fig. 7A–B) [48]. The Cu 2p XPS spectrum (Fig. 7A–C) shows the two peaks centered at 933 and 953 eV were assigned to Cu  $2p_{3/2}$  and Cu  $2p_{1/2}$  present in  $\text{Cu}_2\text{Cl}(\text{OH})_3$ . XPS spectra of spent catalyst was identical clearly indicated that there was no change in oxidation state of  $\text{Cu}^{2+}$  in both fresh and spent catalyst after five recycles (Fig. 8A–C).

$\text{H}_2$ -temperature programmed reduction profile for  $\text{Pd/Cu}_2\text{Cl}(\text{OH})_3$  show presence of two broad peaks between 50 and 200 °C in their TPR diagram, assigned to reduction of Pd ( $\text{Pd}^{2+}$  to Pd). Earlier reports suggest it is due to the reduction of different PdCu species [52–54]. Also peaks between 100 and 200 °C and a small peak between 200 and 250 °C are assigned to  $\alpha$ - and  $\beta$ - peaks due to highly dispersed CuO nanoparticles. Third peak which is extended between 300 and 400 °C corresponds to the reduction of  $\text{Cu}^{2+}$  to Cu as shown in Fig. S3[52–55].

### 3.2. Catalytic results

Catalytic methyl- esterification of alcohols, aldehydes and carboxylic acids were carried out using tert-butylhydroperoxide (TBHP) as

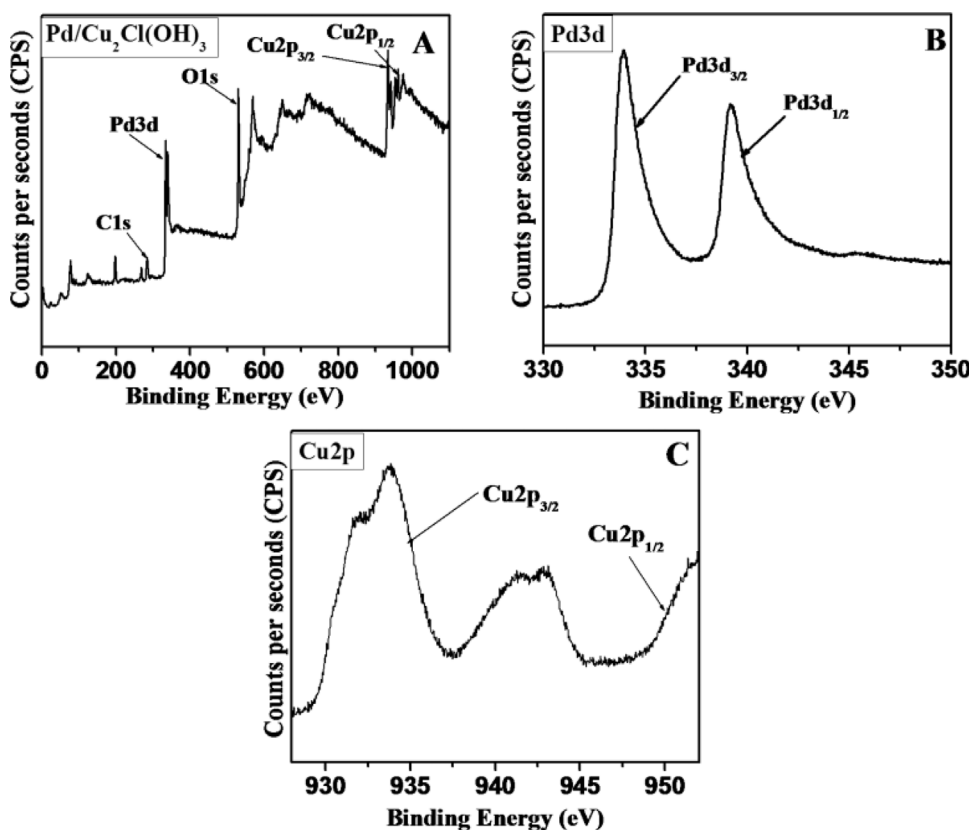


Fig. 7. XPS spectra of survey spectrum of fresh Pd- $\text{Cu}_2\text{Cl}(\text{OH})_3$  (A); Pd 3d (B); Cu 2p (C).

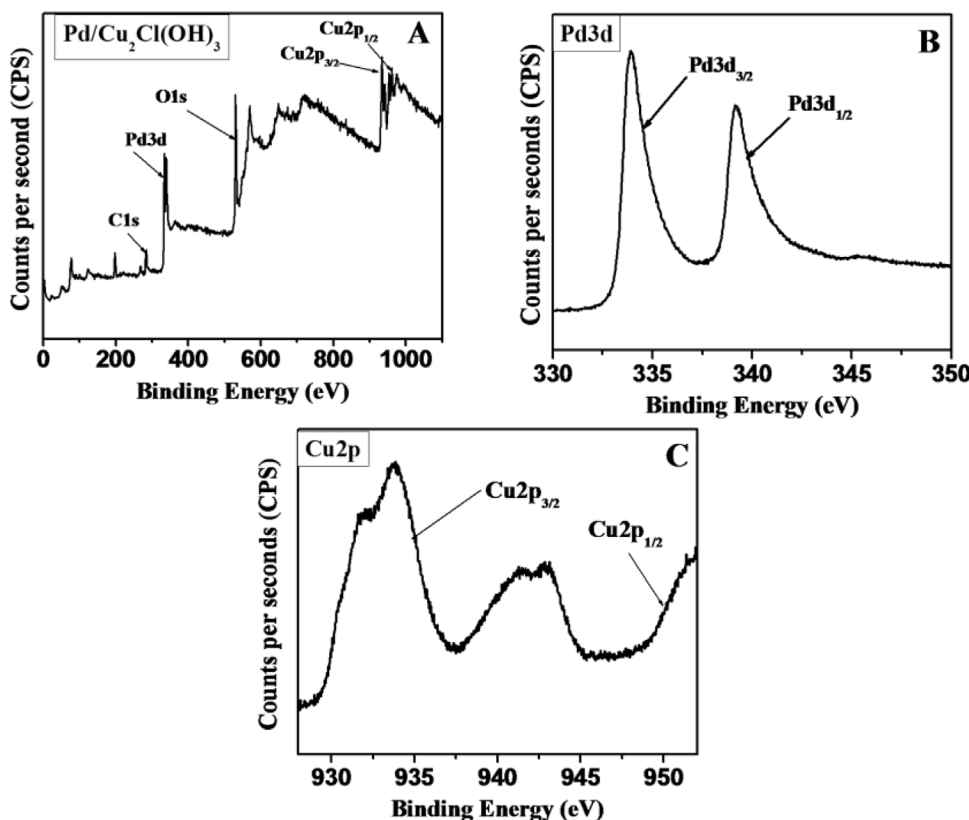
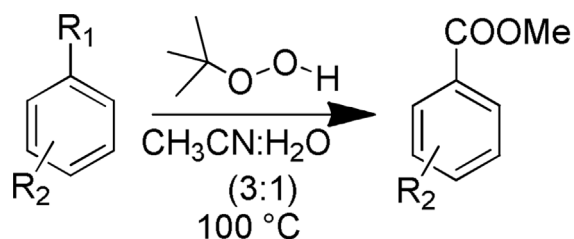


Fig. 8. XPS spectra of survey spectrum of spent Pd- $\text{Cu}_2\text{Cl}(\text{OH})_3$  (A); Pd 3d (B); Cu 2p (C).

oxidizing as well as methylating agents in presence of acetonitrile:water (3:1) as solvent at 100 °C.  $\text{PdCl}_2$ ,  $\text{CuCl}$ ,  $\text{PdCl}_2 + \text{CuO}$  were employed as catalytic materials for methyl esterification reaction (Scheme 2 and

Table 1 and 2). Catalytic methyl-esterification of (4-methoxyphenyl) methanol using  $\text{CuCl}$  as catalyst resulted in complete conversion of the substrate with the formation of methyl-4-methoxybenzoate major



$R_1 = \text{CH}_2\text{OH}$

$R_2 = \text{H, Cl, OMe, and iso-propyl}$

$R_1 = \text{CHO}$

$R_2 = \text{H, Br, NO}_2, \text{OH, Cl, OMe and CN}$

$R_1 = \text{COOH}$

$R_2 = \text{H and NO}_2$

**Scheme 2.** Catalytic methyl-esterification of alcohols, aldehydes and acids using  $\text{PdCl}_2$ ,  $\text{CuCl}$ ,  $\text{PdCl}_2 + \text{CuO}$ ,  $\text{CuO}$  or  $\text{Pd-Cu}_2\text{Cl}(\text{OH})_3$  nanocatalyst and TBHP as oxidizing and methylating agent.

**Table 1**  
Screening of catalysts for methyl-esterification of (4-methoxyphenyl)methanol.

Entry	Catalyst	% Conv.	% Selectivity		
			A	B	C
1 <sup>a</sup>	$\text{CuCl}$	100	66	–	34
2 <sup>b</sup>	$\text{PdCl}_2$	100	27	26	47
3 <sup>c</sup>	$\text{PdCl}_2\text{-CuO}$	99.5	43	45	12

product with 66% selectivity.  $\text{PdCl}_2$  under identical conditions gave 4-methoxybenzoic acid and methyl 4-methoxybenzoate were formed with 26% and 27% selectivity respectively. To determine the role of  $\text{Pd}^{2+}$  and  $\text{Cu}^{2+}$  in the catalytic reaction,  $\text{PdCl}_2$  (4 mg with respect to (4-methoxyphenyl)methanol) and  $\text{CuO}$  (6 mg with respect to (4-methoxyphenyl)methanol) were used as catalyst for aforementioned reaction. 4-methoxybenzoic acid was formed as major product with 45% selectivity. 4-methoxybenzoate was formed as major byproduct with 43% selectivity.

Furthermore, as discussed in the previous sections  $\text{CuO}$  and  $\text{Pd-Cu}_2\text{Cl}(\text{OH})_3$  were used for oxidation of (4-methoxyphenyl)methanol to investigate the role of Pd. Catalytic methyl esterification was carried out using (4-methoxyphenyl)methanol because electron rich benzyl alcohol is the best substrate for methyl-esterification because electron donating group help in stabilizing the  $\text{PhCOO}^\cdot$  free radical, resulting in enhance reactivity with methyl free radical generated during the reaction. Therefore, electron rich benzyl alcohol is best substrate for methyl esterification. In presence of  $\text{CuO}$  nanocatalyst (4-methoxyphenyl)methanol showed 100% conversion with 70% selectivity for methyl 4-methoxybenzoate whereas in presence of  $\text{Pd-Cu}_2\text{Cl}(\text{OH})_3$  nanocatalyst 4-methoxy benzyl alcohol completely converted to methyl 4-methoxybenzoate with 96% selectivity for methyl 4-methoxybenzoate. Thus, further the substrate scope was investigated using  $\text{Pd-Cu}_2\text{Cl}(\text{OH})_3$  nanocatalyst. To examine the scope of methyl esterification reaction several substituted benzylic alcohols were also investigated for the synthesis of methyl esters. The results are summarized in Table 2.  $\text{Pd-Cu}_2\text{Cl}(\text{OH})_3$  nanocatalyst tolerated several steric and electronic substituents of the benzylic alcohols, as well as heterocyclic substrates, all resulting in moderate to excellent yield. Benzaldehyde and substituted

**Table 2**

Catalytic methyl-esterification using TBHP as methylating source and oxidizing agent using  $\text{Pd/Cu}_2\text{Cl}(\text{OH})_3$  heterogeneous catalyst.

Entry	Substrate	% Conv.	(Methyl ester)	% Sel.
Alcohols				
1		100		96
2*		100		70
3		100		93
4		100		72
5		100		71
6		98		44
Aldehydes				
7		100		100
8		100		93
9		100		87
10		100		87
11		100		92
12		100		85

(continued on next page)

Table 2 (continued)

Entry	Substrate	% Conv.	(Methyl ester)	% Sel.
Alcohols				
13		100		64
14		100		41
15		100		30
Carboxylic acids				
16		100		97
17		100		92
18		100		100
Miscellaneous				
19		100		40
20		100		34
21		49		65

benzaldehyde also showed excellent yields for their respective methyl esters. A wide range of functional groups, including  $-Br$ ,  $-Cl$ , cyano, and nitro, all were performed smoothly under the optimized conditions. 2-Hydroxy benzaldehyde showed 30% yield for the corresponding methyl ester. Lower yield for hydroxyl substituted benzaldehyde may be due to its sensitive nature towards oxidants present in the substrate. After the successful application of the oxidative methyl esterification of the alcohols and aldehydes, this methodology was utilized for carboxylic acid since they are cheaper and stable. The benzoic acid and substituted benzoic acids showed better catalytic performance corresponding to alcohols and aldehydes under identical reaction conditions. Five and six-membered heterocyclic compounds were also investigated for methyl-esterification reaction. Pyridin-2-yl methanol under identical reaction condition gave 100% conversions and 40% selectivity for desired methyl picolinate. Benzo[d][1,3]dioxol-5-ylmethanol showed 100% conversion but only 30% selectivity for desired methyl benzo[d][1,3]dioxole-5-carboxylate. Furan-2-carbaldehyde showed 49% conversion and 65% selectivity for methyl furan-2-carboxylate. Alcohols containing heterocyclic moieties were comparatively less active as

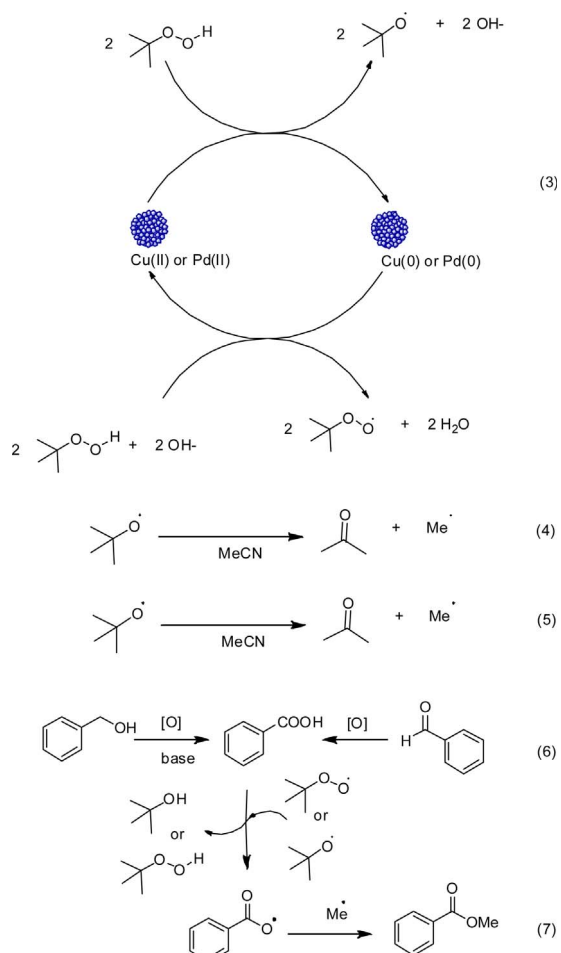


Chart 1. Mechanism for methyl-esterification of benzyl alcohols using CuO or Pd-Cu<sub>2</sub>Cl(OH)<sub>3</sub> nanocatalyst and TBHP as an oxidizing and methylating agent.

compared to non-heterocyclic moieties because they have the tendency to bind to transition metals and can act as catalyst deactivators. Therefore, heterocyclic moieties gave the inferior catalytic performance with Pd/Cu<sub>2</sub>Cl(OH)<sub>3</sub> catalyst.

Reaction conditions: 1 mmol of (4-methoxyphenyl)methanol; 700 mg (8 equivalent) TBHP (70 wt% in H<sub>2</sub>O); CuCl (10 mg with respect to (4-methoxyphenyl)methanol); PdCl<sub>2</sub> (10 mg with respect to (4-methoxyphenyl)methanol); PdCl<sub>2</sub>:CuO (4 mg PdCl<sub>2</sub>: 6 mg CuO with respect to with respect to (4-methoxyphenyl)methanol); K<sub>2</sub>CO<sub>3</sub> (44 mg) in 4 ml CH<sub>3</sub>CN:H<sub>2</sub>O (3:1) heated in 100 °C; time = 24 h, A = methyl-4-methoxybenzoate; B = 4-methoxybenzoic acid; C = others; products were confirmed by GCMS.

Reaction conditions: 1 mmol of substrate; 700 mg (8 equivalent) TBHP (70 wt% in H<sub>2</sub>O); Pd-Cu<sub>2</sub>Cl(OH)<sub>3</sub>(10 mg),\* CuO (10 mg); K<sub>2</sub>CO<sub>3</sub> (44 mg) in 4 ml CH<sub>3</sub>CN:H<sub>2</sub>O (3:1) heated in 100 °C; time = 24 h, products were confirmed by GCMS.

### 3.3. Mechanistic insight into the catalytic methyl esterification

Based on previous literature reports the most plausible mechanism for methyl esterification of organic substrates by using Cu- or Pd-Cu<sub>2</sub>Cl(OH)<sub>3</sub> based catalysis is illustrated in Chart 1[26]. Cu<sup>2+</sup> presents better catalytic performance as compared to other support because Cu<sup>2+</sup> is a superior oxidizing agent with the standard oxidation potential of +0.34 eV. Pd<sup>2+</sup> is still the strong oxidizing agent with the standard oxidation potential of +0.951 eV[56]. Therefore, incorporation of Pd<sup>2+</sup> to the catalytic material further enhances the catalytic performance towards oxidative methyl esterification reaction. The reaction

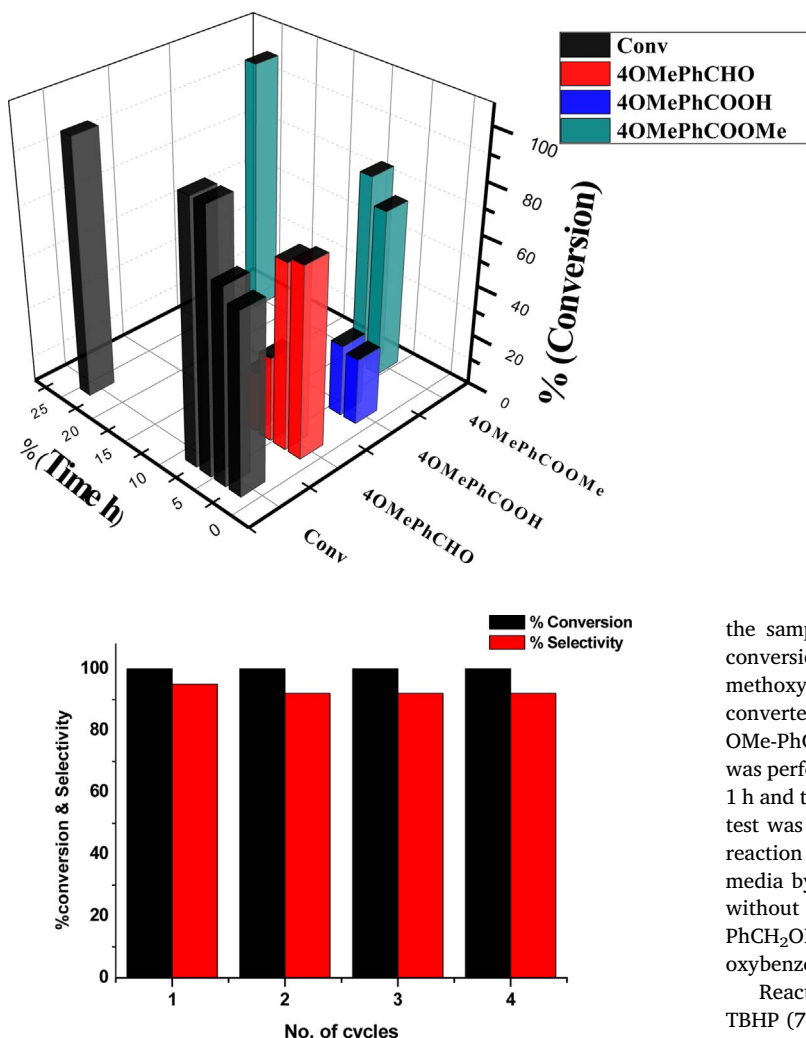


Fig. 9. Kinetic study for catalytic methyl-esterification of 4-OMe-PhCH<sub>2</sub>OH.

initiates with the decomposition of TBHP to generate the *tert*-butoxyl and *tert*-butylperoxy radicals in the presence of Cu- or Pd-Cu<sub>2</sub>Cl(OH)<sub>3</sub> catalyst [57,58]. The alcohols and aldehydes directly oxidized carboxylic acid in the presence of oxidant, base and CuO or Pd-Cu<sub>2</sub>Cl(OH)<sub>3</sub> nanocatalyst. TBHP is activated by Pd or Cu ions present in Pd-Cu<sub>2</sub>Cl(OH)<sub>3</sub> nanocatalyst to form *tert*-butoxyl or butyl peroxy radicals. *In-situ* generated *tert*-butoxyl radical is converted by a simplistic unimolecular mechanism to acetone and a methyl radical [59]. Previously Hix et al. [60] have performed EPR studies to investigate methyl esterification of DNA molecule to form methylated DNA molecule using TBHP molecule as oxidizing agent and methyl source. EPR studies clearly show formation of methyl free radical. They also detected formation of acetone during the reaction. Eventually, the carboxylic acid reacts with *in-situ* generated *tert*-butoxyl or *tert*-butylperoxy radical to form acyloxy radical. The acyloxy radical ultimately reacts with methyl radical resulting into the desired ester.



#### 3.4. Kinetic and recycle study

Kinetic study for catalytic methyl-esterification of 4-OMe-PhCH<sub>2</sub>OH (4-methoxyphenyl)methanol) was performed by periodically injecting

Fig. 10. Recycle study for methyl esterification of (4-methoxyphenyl)methanol using Pd-Cu<sub>2</sub>Cl(OH)<sub>3</sub> nanocatalyst and TBHP as an oxidizing and methylating agent.

the samples into the GC. Kinetic study experiments show complete conversion of 4-OMe-PhCH<sub>2</sub>OH with 76.5% selectivity for methyl 4-methoxybenzoate in 8 h. However 4-OMe-PhCH<sub>2</sub>OH was completely converted into methyl 4-methoxybenzoate in 24 h. Kinetic study for 4-OMe-PhCH<sub>2</sub>OH methyl-esterification is shown in Fig. 9. Leaching study was performed by removing the catalyst from the reaction mixture after 1 h and then continuing the reaction for 24 h without catalyst. Leaching test was carried out using the hot filtration experiment. After 1 h, the reaction was stopped and the catalyst was removed from reaction media by centrifugation and supernatant was allowed to react further without catalyst. Catalyst leaching studies show dip in 4-OMe-PhCH<sub>2</sub>OH (50%) conversion with 3.5% selectivity for methyl 4-methoxybenzoate and 50% selectivity for 4-OMe-PhCHO.

Reaction conditions: 1 mmol of substrate; 700 mg (8 equivalent) TBHP (70 wt% in H<sub>2</sub>O); Pd-Cu<sub>2</sub>Cl(OH)<sub>3</sub>(10 mg); K<sub>2</sub>CO<sub>3</sub> (44 mg) in 4 ml CH<sub>3</sub>CN:H<sub>2</sub>O (3:1) heated in 100 °C; time = 24 h, products were confirmed by GCMS.

Pd-Cu<sub>2</sub>Cl(OH)<sub>3</sub> NPs were also used to check the reusability for methyl esterification of methyl 4-methoxybenzoate. After each reaction cycle, the catalyst was separated by centrifugation and washed with solvent and used for next run. There was no considerable decrease in conversion of methyl 4-methoxybenzoate and methyl 4-methoxybenzoate was formed even after fourth recycle. (Fig. 10)

Reaction conditions: 1 mmol of substrate; 700 mg (8 equivalent) TBHP (70 wt% in H<sub>2</sub>O); Pd-Cu<sub>2</sub>Cl(OH)<sub>3</sub>(10 mg); K<sub>2</sub>CO<sub>3</sub> (44 mg) in 4 ml CH<sub>3</sub>CN:H<sub>2</sub>O (3:1) heated in 100 °C; time = 24 h, products were confirmed by GCMS.

#### 4. Conclusions

To summarize methyl-esterification of various substituted alcohols, aldehydes and carboxylic acids were carried out using *tert*-butylhydroperoxide(TBHP) which act as an oxidizing as well as the methylating agent using CuO or Pd/Cu<sub>2</sub>Cl(OH)<sub>3</sub> nanocatalysts. CuO or Pd/Cu<sub>2</sub>Cl(OH)<sub>3</sub> NPs were synthesized by wet chemical method of CuCl and PdCl<sub>2</sub> by using green solvent “water”. HRTEM of as-prepared CuO materials showed a cube-shaped NPs. HRTEM showed the formation of spherical Pd nanoparticles dispersed on Cu<sub>2</sub>Cl(OH)<sub>3</sub> surface. Using more amount of substrates with less amount of nanocatalyst Pd/Cu<sub>2</sub>Cl(OH)<sub>3</sub> showed excellent catalytic performance with high conversions and selectivity towards aldehydes, alcohols and carboxylic acids for their respective desired methyl esters.

## Acknowledgements

SMM thanks SERB-DST, New Delhi (Project No. EMR/2016/001113) and IIT Indore for funding. We are also grateful to Mrs. Reshma S. Kokane from CSIR National Chemical Laboratory (NCL) Pune providing TEM data. We would also like to acknowledge to Advanced Center for Materials Science (ACMS) for XPS, IIT Kanpur. T.G. and A.M. are grateful to MHRD, Government of India for research fellowship and authors are thankful to SIC, IIT Indore for providing the characterization facility.

## Appendix A. Supplementary data

Supplementary data associated with this article can be found, in the online version, at <https://doi.org/10.1016/j.apcatb.2017.12.056>.

SEM; EDAX, elemental mapping (Fig. S1-S3 and Table S1) and GC-MS data (Spectra:S1-S23) and NMR (Spectra: S24-25) can be accessed from supporting information.

## References

- [1] G. Yan, A.J. Borah, L. Wang, M. Yang, Recent advances in transition metal-catalyzed methylation reactions, *Adv. Synth. Catal.* 357 (2015) 1333–1350.
- [2] E.J. Barreiro, A.E. Kümmerle, C.A.M. Fraga, The methylation effect in medicinal chemistry, *Chem. Rev.* 111 (2011) 5215–5246.
- [3] Q. Zhang, W.A. Van Der Donk, W. Liu, Radical-mediated enzymatic methylation: a tale of two SAMS, *Acc. Chem. Res.* 45 (2012) 555–564.
- [4] J. Chatterjee, F. Rechenmacher, H. Kessler, N-methylation of peptides and proteins: an important element for modulating biological functions, *Angew. Chem. Int. Ed.* 52 (2013) 254–269.
- [5] M.K. Walker-Simmons, P.A. Rose, A.C. Shaw, S.R. Abrams, The 7'-methyl group of abscisic acid is critical for biological activity in wheat embryo germination, *Plant Physiol.* 106 (1994) 1279–1284.
- [6] W.-C. Shieh, S. Dell, O. Repić, 1, 8-diazabicyclo[5.4.0]undec-7-ene (DBU) and microwave-accelerated green chemistry in methylation of phenols, indoles, and benzimidazoles with dimethyl carbonate, *Org. Lett.* 3 (2001) 4279–4281.
- [7] P. Li, J. Zhao, R. Lang, C. Xia, F. Li, Copper-catalyzed methyl esterification of aromatic aldehydes and benzoic alcohols by TBHP as both oxidant and methyl source, *Tetrahedron Lett.* 55 (2014) 390–393.
- [8] B. Liu, F. Hu, B.-F. Shi, Recent advances on ester synthesis via transition-metal catalyzed CH functionalization, *ACS Catal.* 5 (2015) 1863–1881.
- [9] J. Otera, Transesterification, *Chem. Rev.* 93 (1993) 1449–1470.
- [10] C. Liu, S. Tang, L. Zheng, D. Liu, H. Zhang, A. Lei, Covalently bound benzyl ligand promotes selective palladium-catalyzed oxidative esterification of aldehydes with alcohols, *Angew. Chem. Int. Ed.* 51 (2012) 5662–5666.
- [11] S. Gowrisankar, H. Neumann, M. Beller, General and selective palladium-catalyzed oxidative esterification of alcohols, *Angew. Chem. Int. Ed.* 50 (2011) 5139–5143.
- [12] K. Ekoue-Kovi, C. wolf, One-pot Oxidative esterification and amidation of aldehydes, *Chem. Eur. J.* 14 (2008) 6302–6315.
- [13] W.-J. Yoo, C.-J. Li, Copper-catalyzed oxidative esterification of alcohols with aldehydes activated by lewis acids, *Tetrahedron Lett.* 48 (2007) 1033–1035.
- [14] B. Xu, X. Liu, J. Haubrich, C.M. Friend, Vapour-Phase gold-surface-mediated coupling of aldehydes with methanol, *Nat. Chem.* 2 (2010) 61–65.
- [15] W.-J. Yoo, C.-J. Li, Highly stereoselective oxidative esterification of aldehydes with  $\beta$ -dicarbonyl compounds, *J. Org. Chem.* 71 (2006) 6266–6268.
- [16] H. Miyamura, T. Yasukawa, S. Kobayashi, Aerobic oxidative esterification of alcohols catalyzed by polymer-incarcerated gold nanoclusters under ambient conditions, *Green Chem.* 12 (2010) 776–778.
- [17] F.-Z. Su, J. Ni, H. Sun, Y. Cao, H.-Y. He, K.-N. Fan, Gold supported on nanocrystalline  $\beta$ -Ga<sub>2</sub>O<sub>3</sub> as a versatile bifunctional catalyst for facile oxidative transformation of alcohols, aldehydes, and acetals into esters, *Chem. Eur. J.* 14 (2008) 7131–7135.
- [18] S. Kegnaes, J. Mielby, U.V. Mentzel, T. Jensen, P. Fristrup, A. Riisager, One-pot synthesis of amides by aerobic oxidative coupling of alcohols or aldehydes with amines using supported gold and base as catalysts, *Chem. Commun.* 48 (2012) 2427–2429.
- [19] X.-F. Bai, F. Ye, L.-S. Zheng, G.-Q. Lai, C.-G. Xia, L.-W. Xu, Hydrosilane and bismuth-accelerated palladium catalyzed aerobic oxidative esterification of benzylic alcohols with air, *Chem. Commun.* 48 (2012) 8592–8594.
- [20] T. Seki, T. Nakajo, M. Onaka, The Tishchenko reaction: a classic and practical tool for ester synthesis, *Chem. Lett.* 35 (2006) 824–829.
- [21] C.E. Houlden, C.D. Bailey, J.G. Ford, M.R. Gagné, G.C. Lloyd-Jones, K.I. Booker-Milburn, Distinct reactivity of Pd(OTs)<sub>2</sub>: the intermolecular Pd(II)-Catalyzed 1,2-carboamination of dienes, *J. Am. Chem. Soc.* 130 (2008) 10066–10067.
- [22] T. Kochi, S. Urano, H. Seki, E. Mizushima, M. Sato, F. Kakiuchi, Ruthenium-catalyzed amino- and alkoxycarbonylations with carbamoyl chlorides and alkyl chloroformates via aromatic C-H bond cleavage, *J. Am. Chem. Soc.* 131 (2009) 2792–2793.
- [23] W. Zhou, P. Li, Y. Zhang, L. Wang, Palladium-catalyzed direct alkoxycarbonylation of aromatic C-H bonds via selective C-C cleavage of  $\alpha$ -keto esters, *Adv. Synth. Catal.* 355 (2013) 2343–2352.
- [24] K. Sasano, J. Takaya, N. Iwasawa, Palladium(II)-catalyzed direct carboxylation of alkenyl CH bonds with CO<sub>2</sub>, *J. Am. Chem. Soc.* 135 (2013) 10954–10957.
- [25] G. Liao, X.-S. Yin, K. Chen, Q. Zhang, S.-Q. Zhang, B.-F. Shi, Stereoselective alkoxycarbonylation of unactivated C(sp<sup>3</sup>)-H bonds with alkyl chloroformates via Pd (II)/Pd (IV) catalysis, *Nat. Commun.* 7 (2016) 12901.
- [26] Y. Zhu, H. Yan, L. Lu, D. Liu, G. Rong, J. Mao, Copper-catalyzed methyl esterification reactions via C-C bond cleavage, *J. Org. Chem.* 78 (2013) 9898–9905.
- [27] R.A. Molla, M.A. Iqbal, K. Ghosh, S. Kamaluddin, M. Islam, Nitrogen enriched mesoporous organic polymer anchored copper(II) material: an efficient and reusable catalyst for the synthesis of esters and amides from aromatic systems, *Dalton Trans.* 44 (2015) 6546–6559.
- [28] M.B. Gawande, A. Goswami, F.-X. Felpin, T. Asefa, X. Huang, R. Silva, X. Zou, R. Zboril, R.S. Varma, Cu and Cu-based nanoparticles: synthesis and applications in catalysis, *Chem. Rev.* 116 (2016) 3722–3811.
- [29] D. Mott, J. Galkowski, L. Wang, J. Luo, C.-J. Zhong, Synthesis of size-controlled and shaped copper nanoparticles, *Langmuir* 23 (2007) 5740–5745.
- [30] R. Venkatasubramanian, J. He, M.W. Johnson, I. Stern, D.H. Kim, N.S. Pesika, Additive-mediated electrochemical synthesis of platelike copper crystals for methanol electrooxidation, *Langmuir* 29 (2013) 13135–13139.
- [31] Y. Shimotsuma, T. Yuasa, H. Homma, M. Sakakura, A. Nakao, K. Miura, K. Hirao, M. Kawasaki, J. Qiu, P.G. Kazansky, Photoconversion of copper flakes to nanowires with ultrashort pulse laser irradiation, *Chem. Mater.* 19 (2007) 1206–1208.
- [32] R.V. Kumar, Y. Mastai, Y. Diamant, A. Gedanken, Sonochemical synthesis of amorphous Cu and nanocrystalline Cu<sub>2</sub>O embedded in a polyaniline matrix, *J. Mater. Chem.* 11 (2001) 1209–1213.
- [33] M. Salavati-Niasari, N. Mir, F. Davar, A Novel precursor for synthesis of metallic copper nanocrystals by thermal decomposition approach, *Appl. Surf. Sci.* 256 (2010) 4003–4008.
- [34] R. Jin, Y. Yang, Y. Xing, L. Chen, S. Song, R. Jin, Facile synthesis and properties of hierarchical double-walled copper silicate hollow nanofibers assembled by nanotubes, *ACS Nano* 8 (2014) 3664–3670.
- [35] C.-H. Lu, C.-H. Lee, C.-H. Wu, Microemulsion-mediated solvothermal synthesis of copper indium diselenide powders, *Sol. Energy Mat. Sol. Cells* 94 (2010) 1622–1626.
- [36] B. Zhang, Y. Yuan, K. Philippot, N. Yan, Ag-Pd and CuO-Pd nanoparticles in a hydroxyl group functionalized ionic liquid: synthesis, characterization and catalytic performance, *Catal. Sci. Techn.* 5 (2015) 1683–1692.
- [37] X. Song, S. Sun, W. Zhang, Z. Yin, A Method for the synthesis of spherical copper nanoparticles in the organic phase, *J. Colloid Interface Sci.* 273 (2004) 463–469.
- [38] W. Songping, M. Shuyuan, Preparation of micron size copper powder with chemical reduction method, *Mater. Lett.* 60 (2006) 2438–2442.
- [39] J. Xiong, Y. Wang, Q. Xue, X. Wu, Synthesis of highly stable dispersions of nano-sized copper particles using L-ascorbic acid, *Green Chem.* 13 (2011) 900–904.
- [40] U.S. Shenoy, A.N. Shetty, A simple solution phase synthesis of copper nanofluid using single-step glucose reduction method, *Synth. React. Inorg. Met.-Org. Nano-Metal.* 43 (2013) 343–348.
- [41] M. Poliakoff, P. Anastas, A principled stance, *Nature* 413 (2001) 257–258.
- [42] J.M. DeSimone, Practical approaches to green solvents, *Science* 297 (2002) 799–803.
- [43] S.L.Y. Tang, R.L. Smith, M. Poliakoff, Principles of green chemistry: productively, *Green Chem.* 7 (2005) 761–762.
- [44] B. Zhao, P. Liu, H. Zhuang, Z. Jiao, T. Fang, W. Xu, B. Lu, Y. Jiang, Hierarchical self-assembly of microscale leaf-like CuO on graphene sheets for high-performance electrochemical capacitors, *J. Mater. Chem. A* 1 (2013) 367–373.
- [45] A.-X. Yin, X.-Q. Min, W. Zhu, W.-C. Liu, Y.-W. Zhang, C.-H. Yan, Pt-Cu and Pt-Pd-Cu concave nanocubes with high-index facets and superior electrocatalytic activity, *Chem. Eur. J.* 18 (2012) 777–782.
- [46] A.-X. Yin, X.-Q. Min, W. Zhu, H.-S. Wu, Y.-W. Zhang, C.-H. Yan, Multiply twinned Pt-Pd nanoicosahedrons as highly active electrocatalysts for methanol oxidation, *Chem. Commun.* 48 (2012) 543–545.
- [47] X. Du, H.-Y. Li, J. Yu, X. Xiao, Z. Shi, D. Mao, G. Lu, Realization of a highly effective Pd-Cu-Cl<sub>x</sub>/Al<sub>2</sub>O<sub>3</sub> catalyst for low temperature CuO oxidation by pre-synthesizing the active copper phase of Cu<sub>2</sub>Cl(OH)<sub>3</sub>, *Catal. Sci. Techn.* 5 (2015) 3970–3979.
- [48] G. Hu, F. Nitze, T. Sharifi, H.R. Barzegar, T. Wågberg, Self-assembled palladium nanocrystals on helical carbon nanofibers as enhanced electrocatalysts for electro-oxidation of small molecules, *J. Mater. Chem.* 22 (2012) 8541–8548.
- [49] S. Wolf, C. Feldmann, Cu<sub>2</sub>X(OH)<sub>3</sub> (X = Cl<sup>-</sup>, NO<sub>3</sub><sup>-</sup>): Synthesis of nanoparticles and its application for room temperature deposition/printing of conductive copper thin-films, *J. Mater. Chem.* 20 (2010) 7694–7699.
- [50] W. Wei, P. Gao, J. Xie, S. Zong, H. Cui, X. Yue, Uniform Cu<sub>2</sub>Cl(OH)<sub>3</sub> hierarchical microspheres: a novel adsorbent for methylene blue adsorptive removal from aqueous solution, *J. Solid State Chem.* 204 (2013) 305–313.
- [51] S. Tada, M. Yokoyama, R. Kikuchi, T. Haneda, H. Kameyama, N<sub>2</sub>O pulse titration of Ni- $\alpha$ -Al<sub>2</sub>O<sub>3</sub> catalysts: a new technique applicable to nickel surface-area determination of nickel-based catalysts, *J. Phys. Chem. C* 117 (2013) 14652–14658.
- [52] J. Sá, H. Vinek, Catalytic hydrogenation of nitrates in water over a bimetallic catalyst, *Appl. Catal. B* 57 (2005) 247–256.
- [53] D. Gašparovičová, M. Králik, M. Hronec, Z. Vallušová, H. Vinek, B. Corain, Supported Pd–Cu catalysts in the water phase reduction of nitrates: functional resin versus alumina, *J. Mol. Catal. A: Chem.* 264 (2007) 93–102.
- [54] M.A. Jaworski, I. D. lick, G. J. siri, M. L. casella, ZrO<sub>2</sub>-modified Al<sub>2</sub>O<sub>3</sub>-supported PdCu catalysts for the water denitrification reaction, *Appl. Catal. B- Environ.* 156–157 (2014) 53–61.
- [55] H.-d. Zhuang, S. -f. Bai, X. -m. Liu, Z. -f. Yan, Structure and performance of Cu/ZrO<sub>2</sub>

catalyst for the synthesis of methanol from CO<sub>2</sub> hydrogenation, *J. Fuel Chem. Technol.* 38 (2010) 462–467.

[56] W.M. Haynes, CRC Handbook of Chemistry and Physics, CRC press, 2014.

[57] L. Chen, E. Shi, Z. Liu, S. Chen, W. Wei, H. Li, K. Xu, X. Wan, Bu4NI-catalyzed C–O bond formation by using a cross-dehydrogenative coupling (CDC) reaction, *Chem. Eur. J.* 17 (2011) 4085–4089.

[58] Z. Liu, J. Zhang, S. Chen, E. Shi, Y. Xu, X. Wan, Cross coupling of acyl and aminyl radicals: direct synthesis of amides catalyzed by Bu4NI with TBHP as an oxidant, *Angew. Chem. Int. Ed.* 51 (2012) 3231–3235.

[59] R.T. Gephart I.I.I., C.L. McMullin, N.G. Sapiezyński, E.S. Jang, M.J.B. Aguila, T.R. Cundari, T. H. Warren, Reaction of Cu<sup>1</sup> with dialkyl peroxides: Cu<sup>II</sup>-alkoxides, alkoxy radicals, and catalytic CH etherification, *J. Am. Chem. Soc.* 134 (2012) 17350–17353.

[60] S. Hix, O. Augusto, DNA methylation by tert-butyl hydroperoxide-iron (II): a role for the transition metal ion in the production of DNA base adducts, *Chem. Biol. Interact.* 118 (1999) 141–149.